2024 European Control Conference (ECC)
June 25-28, 2024. Stockholm, Sweden

Pitot tube measure-aided air velocity and attitude estimation in GNSS denied environment

Tomas L. de Oliveira, Pieter van Goor, Tarek Hamel, Robert Mahony and Claude Samson

***Abstract*— This paper addresses the problem of estimating air velocity and gravity direction for small autonomous fixed-wing drones in GNSS[1]-denied environments. The proposed solution uses a minimal sensor suite, relying on Pitot tube measurements and Inertial Measurement Unit (IMU) signals, including only gyrometers and accelerometers. The approach combines the Riccati observer and Equivariant Filter designs, using an over-parametrization technique to design an observer on $\mathbf{SO}(3) \times \mathbb{R}^3$ and subsequently re-project to $\mathcal{S}^2 \times \mathbb{R}^3$ to estimate the gravity direction. The system's observability is analyzed, and local exponential stability of the origin of the observer error is demonstrated as long as the aircraft attitude is persistently exciting. The observer was evaluated using real flight data from an indoor experiment to showcase the estimator's performance.**

I. INTRODUCTION

Airspeed-aided air velocity and attitude estimation is critical for the control of fixed-wing aerial vehicles.

Good performance and safety often rely on accurate estimation of the gravitational direction and estimation (or measurement) quality of the air-velocity vector relative to the body fixed-frame. Large aircraft are equipped with sophisticated and well-calibrated air data systems that measure the aircraft's air velocity relative to the body-fixed frame. However, the standard air sensors that are available on most scale-model fixed-wing aircraft provide only a partial measurement of the air velocity vector. The most common of these is the Pitot tube, which is typically aligned with the aircraft's longitudinal axis and provides a component of the air velocity in that vector.

There is abundant literature on attitude and air velocity filtering techniques. Popular approaches to attitude estimation from the last 20 years rely on IMU signals, including gyroscope, accelerometer, and sometimes magnetometer measurements (see [1], [2], [3], [4]). They typically assume that the accelerometer signal is dominated by the gravity vector. While this assumption has proven useful in many practical situations, it is unreliable for a fixed-wing aircraft experiencing large accelerations when sharply changing direction or making turns at high speeds. To overcome this problem, several authors have incorporated body-fixed velocity measurements provided by an onboard Doppler radar or inertial-frame measurements of the vehicle's velocity provided by a GNSS receiver. Estimating the attitude of a vehicle using velocity measurements is referred to as the velocity-aided attitude (VAA) problem. Velocity-aided attitude estimation algorithms typically include an estimator for the vehicle velocity which acts as an auxiliary state and provides additional information for the primary estimate of the vehicle attitude [5], [6], [7], [8], [9].

As for the air velocity estimation, most early work exploits IMU, GNSS inertial velocity, Pitot tube measurements, and vehicle dynamics models to estimate the airspeed and the air velocity direction in the body-fixed frame [10], [11]. This model-based approach requires accurate dynamic models of fixed-wing aircraft and, hence, a good description of the aerodynamic forces and moments, which are very difficult to obtain in practice for small UAVs. The lack of accurate information on the control inputs poses another difficulty, as highlighted in [10]. Several authors propose model-free solutions for attitude and air velocity estimation. These solutions rely only on measurements from a GNSS receiver, an IMU, and a Pitot tube and assume that the ambient wind is constant (gusts are considered as disturbances) [12], [13]. The key idea in these papers is to design a velocity-aided attitude estimator using an extended Kalman filter followed by a Kalman filter for wind estimation. The system's observability is analyzed in both papers, and solutions were validated using experimental data.

Solutions considering air velocity and attitude estimation from only IMU and Pitot tube data are few. In [14], a nonlinear complementary filter is proposed. It implicitly assumes that the acceleration in the aircraft body-fixed frame is negligible and the side-slip angle is zero.

The present paper considers the airspeed-aided attitude estimation without magnetometer and GNSS measurements. The design procedure is based on the deterministic Riccati observer design framework proposed in [15] and the Equivariant filter proposed in [16]. Observability conditions under which local exponential stability is guaranteed have been identified. Finally, experimental results demonstrate the efficiency of the proposed solution within a large attraction domain.

The paper is structured into six sections, including the introduction and conclusion. Section II briefly describes the notation and math related to the design of the proposed observers. Section III describes the Airspeed-aided attitude

This work was supported by the Franco-Australian International Research Project "Advancing Autonomy for Unmanned Robotic Systems" (IRP ARS).

T. L. de Oliveira and C. Samson are with I3S (University Cote d'Azur, CNRS, Sophia Antipolis) (tlopes@i3s.unice.fr; samson@i3s.unice.fr)

P. van Goor and R. Mahony are with the Systems Theory and Robotics Group Australian National University ACT, 2601, Australia (pieter.vanGoor@anu.edu.au; robert.Mahony@anu.edu.au)

T. Hamel is with I3S-UniCA-CNRS, University Cote d'Azur Sophia Antipolis and the Insitut Universitaire de France (thamel@i3s.unice.fr)

[1]Global Navigation Satellite Systems

Copyright ©2024 EUCA

problem and observability issues. In Section IV a nonlinear Riccati observer design is proposed and analyzed. Section V presents some results supporting the proposed approach using a real-world flight data set.

II. Preliminary material

- $\mathcal{I} = \{O, e_1, e_2, e_3\}$ denotes a North-East-Down (NED) right-handed inertial frame with a fixed origin O and the canonical basis of $\mathbb{R}^3$ with e_3 pointing downwards. $\mathcal{B} = \{G, e_1^{\mathcal{B}}, e_2^{\mathcal{B}}, e_3^{\mathcal{B}}\}$ is the body-fixed frame with the origin G placed at the vehicle center of mass, and the vector $e_1^{\mathcal{B}}$ aligned with the vehicle longitudinal axis, pointing forward.
- $|x|$ denotes the Euclidean norm of $x \in \mathbb{R}^n$, and x_i denotes its *ith* component.
- For any vector $z := (z_1, z_2, z_3) \in \mathbb{R}^3$, $z^\times$ denotes the skew-symmetric matrix associated with the cross product given by

$$z^\times = \begin{bmatrix} 0 & -z_3 & z_2 \\ z_3 & 0 & -z_1 \\ -z_2 & z_1 & 0 \end{bmatrix}.$$

- $\mathcal{S}^2 := \{v \in \mathbb{R}^3 \mid |v| = 1\}$ denotes the unit 2-sphere.
- $\mathbf{SO}(3)$ denotes the special orthogonal group and is the Lie group of 3D rotations, defined as

$$\mathbf{SO}(3) := \{R \in \mathbb{R}^{3\times 3} \mid R^\top R = I_3,\ \det(R) = 1\}.$$

The Lie algebra of this group is denoted

$$\mathfrak{so}(3) := \{\Omega^\times \in \mathbb{R}^{3\times 3} \mid \Omega \in \mathbb{R}^3\}.$$

- s_γ and c_γ represent the trigonometric functions $\sin(\gamma)$ and $\cos(\gamma)$, respectively.
- The set of symmetric positive-definite matrices of dimension n is denoted $\mathbb{S}_+(n)$.
- With f denoting a vector-valued function depending on the two variables x and y, and on the time variable t, we write $f = O(|x|^{k_1}|y|^{k_2})$ with $k_1 \geq 0$ and $k_2 \geq 0$ if $\forall t : |f(x, y, t)|/(|x|^{k_1}|y|^{k_2}) \leq \gamma < \infty$ in the neighbourhood of $(x = 0, y = 0)$. If f depends only on x and t then we write $f(x, t) = O(|x|^k)$ if $\forall t : |f(x, t)|/|x|^k \leq \gamma < \infty$ in the neighbourhood of $x = 0$.

A. Definitions and Conditions of Observability

Consider the following generic linear time-varying (LTV) system[2]

$$\begin{cases} \dot{x} = A(t)x + B(t)u \\ y = C(t)x \end{cases} \tag{1}$$

where $x \in \mathbb{R}^n$ is the state, $u \in \mathbb{R}^s$ is the input and $y \in \mathbb{R}^m$ is the output of the system. $A(t)$, $B(t)$, $C(t)$ are finite-dimensional continuous and bounded matrix-valued functions. The following definitions and properties of observability of an LTV system are recalled from [17], [15].

[2]The time dependence has been omitted from the state variables for brevity, while deliberately retained for matrices A, B, and C to highlight the system's time-varying nature.

Definition 1 (Uniform Observability): The system (1) is called *uniformly observable* if there exist $\delta, \mu > 0$ such that, for all $t \geq 0$,

$$W(t, t + \delta) \geq \mu I_n > 0 \tag{2}$$

with

$$W(t, t + \delta) \triangleq \frac{1}{\delta} \int_t^{t+\delta} \Phi^\top(s, t) C^\top(s) C(s) \Phi(s, t) ds,$$

where $\Phi(s, t)$ is the transition matrix associated with $A(t)$:

$$\frac{d}{dt}\Phi(s, t) = A(t)\Phi(s, t) \qquad \Phi(t, t) = I_n.$$

The matrix-valued function $W(t, t + \delta)$ is called the *observability Gramian* of System (1). When (2) is satisfied, one also says that the pair $(A(t), C(t))$ is uniformly observable. Checking the uniform observability directly from the Gramian is tedious and typically very challenging. The following valuable and lesser-known lemma highlights a sufficient condition for uniform observability that will be instrumental in this paper.

Lemma 1 ([15]): If

1) $C(t) = \Pi(t)\bar{C}$ with $\bar{C}$ a constant matrix,
2) A is constant and such that the pair $(A, \bar{C})$ is Kalman observable,
3) all eigenvalues of A are real,
4) $\Pi(t)$ is persistently exciting, that is, there exists $\bar{\delta}, \bar{\mu} > 0$ such that, $\forall t \geq 0$:

$$M(t, t + \bar{\delta}) \triangleq \frac{1}{\bar{\delta}} \int_t^{t+\bar{\delta}} \Pi^\top(s)\Pi(s) ds \geq \bar{\mu} I > 0 \tag{3}$$

then the observability Gramian of System (1) satisfies the condition (2).

III. Problem description

Consider the aircraft with body-fixed frame $\mathcal{B}$. Let the matrix $R \in \mathbf{SO}(3)$ encode the vehicle attitude with respect to the inertial frame $\mathcal{I}$. Let $v, V \in \mathbb{R}^3$ denote the vector of coordinates of the vehicle's inertial and body-fixed velocities, respectively. That is, v denotes the velocity of the origin of $\mathcal{B}$ with respect to $\mathcal{I}$ expressed in $\mathcal{I}$, and $V = R^\top v$ denotes this expression in $\mathcal{B}$.

Let $v_w \in \mathbb{R}^3$ denote the vector of coordinates of the ambient wind velocity expressed in $\mathcal{I}$. The vector of coordinates of the aircraft air-velocity expressed in the frame $\mathcal{I}$ is given by $v_a = v - v_w$. Its expression in the body-fixed frame $\mathcal{B}$ is denoted $V_a = R^\top v_a$. Suppose that the vehicle is equipped with an IMU, providing 3-axis measurements of the vehicle's specific acceleration $a \in \mathbb{R}^3$ and angular velocity $\Omega \in \mathbb{R}^3$, both expressed in coordinates of the body-fixed frame $\mathcal{B}$. The kinematic equations expressing the motion of the vehicle in Earth's gravitational field are thus given by

$$\dot{R} = R\Omega^\times,$$
$$\dot{v} = ge_3 + Ra.$$

Assuming that v_w is constant or slowly time-varying and bounded ($\dot{v}_w \approx 0$), one verifies the v_a inherits the same

dynamics of v, and hence

$$\dot{R} = R\Omega^{\times}, \tag{4a}$$
$$\dot{v}_a = ge_3 + Ra. \tag{4b}$$

Assume that the aircraft is equipped with a calibrated single or multiprobe Pitot tube placed at G, which provides (via pressure sensing) the component $y_{\mathrm{a},i}$ of V_a along the body-fixed direction $b_i \in \mathcal{S}^2$, of each probe, where $i = 1, \ldots, m$:

$$y_{\mathrm{a}} = \begin{pmatrix} y_{\mathrm{a},1} \\ \vdots \\ y_{\mathrm{a},m} \end{pmatrix} = \begin{pmatrix} b_1^{\top} \\ \vdots \\ b_m^{\top} \end{pmatrix} R^{\top} v_a = B^{\top} R^{\top} v_a. \tag{5}$$

Note that in the standard setup for small fixed-wing UAVs, a single Pitot tube ($m = 1$) is installed along the forward axis, resulting in the relationship $B = e_1 \in \mathbb{R}^{3\times 1}$.

A. Non-observability of (4)- (5)

To show that the system state (R, v_a) of (4) and (5) is not observable, we will exploit the following invariance notion.

Definition 2 (Invariance and output indistinguishability): Let the state space $\mathcal{M}$ and the output spaces $\mathcal{N}_i$ for $i = 1, \ldots, m$ be finite-dimensional smooth manifolds. Let the velocity space $\mathbb{L}$ be a finite-dimensional real vector space. Consider the nonlinear system

$$\dot{\xi} = f(\xi, u), \tag{6a}$$
$$y_i = h_i(\xi), \tag{6b}$$

with $\xi \in \mathcal{M}$, $u \in \mathbb{L}$, and $y_i \in \mathcal{N}_i$. The system dynamics (6) is said to be *invariant* to a closed family of invertible and differentiable functions $\alpha_S : \mathcal{M} \to \mathcal{M}$ if

$$\forall S \in \mathbf{G}, \quad \frac{\mathrm{d}}{\mathrm{d}t}\alpha_S(\xi) = f(\alpha_S(\xi), u), \tag{7}$$

with $\mathbf{G}$ the parameter space indexing α_S. It is further said output indistinguishable if:

$$\forall S \in \mathbf{G}, \quad h_i(\alpha_S(\xi)) = h_i(\xi). \tag{8}$$

The satisfaction of definitions (7)-(8) implies that any trajectory $\xi(t)$ of a system is indistinguishable from $\xi'(t) = \alpha_S(\xi(t))$ for any $S \in \mathbf{G}$. This means that, at best, one can determine a system trajectory $\xi(t)$ up to an equivalence class of trajectories $[\xi(t)] = \{\xi'(t) = \alpha_S(\xi(t)) \mid S \in \mathbf{G}\}$.

Theorem 1: Consider the system dynamics (4) along with (5). Let $\xi := (R, v_a) \in \mathbf{SO(3)} \times \mathbb{R}^3$, $u := (\Omega, a) \in \mathbb{R}^3 \times \mathbb{R}^3$, $y_i := y_{\mathrm{a},i} \in \mathbb{R}$, and

$$f((R, v_a), (\Omega, a)) := (R\Omega^{\times}, ge_3 + Ra) \tag{9a}$$
$$h_i(R, v_a) := b_i^{\top} R^{\top} v_a \tag{9b}$$

Define $\alpha_{S_{e_3}} : \mathbf{SO(3)} \times \mathbb{R}^3 \to \mathbf{SO(3)} \times \mathbb{R}^3$ as

$$\alpha_{S_{e_3}}(R, v_a) := (S_{e_3}R, S_{e_3}v_a),$$

with $S_{e_3} = S_{e_3}(\theta) \in \mathbf{SO}(3)$ any rotation of an angle θ about the axis e_3 (i.e. $S_{e_3}e_3 = e_3$). Then the system (9) is invariant and output indistinguishable to every $\alpha_{S_{e_3}}$.

Proof: To verify the invariance of the dynamics (7), one computes

$$\begin{aligned} &\frac{\mathrm{d}}{\mathrm{d}t}\alpha_{S_{e_3}}(R, v_a) = (S_{e_3}R\Omega^{\times}, S_{e_3}(ge_3 + Ra)) \\ &= ((S_{e_3}R)\Omega^{\times}, ge_3 + (S_{e_3}R)a) \\ &= f((S_{e_3}R, S_{e_3}v_a), (\Omega, a)) = f(\alpha_{S_{e_3}}(R, v_a), (\Omega, a)). \end{aligned}$$

Likewise, to verify the measure equation is output indistinguishable in the sense of (8), one computes

$$\begin{aligned} h_i(\alpha_{S_{e_3}}(R, v_a)) &= h_i(S_{e_3}R, S_{e_3}v_a), \\ &= b_i^{\top}(S_{e_3}R)^{\top}(S_{e_3}v_a) = h_i(R, v_a). \end{aligned}$$

This completes the proof. ∎

Recognizing that the complete state representation of (R, v_a) is not observable, we reframe the problem by focusing solely on observable state components. This entails designing an observer for the vehicle's gravitational direction, denoted as $\eta := R^{\top}e_3$ (involving the pitch and roll angles of the aircraft), and the air velocity $V_a = R^{\top}v_a$ in the body-fixed reference frame:

$$\dot{\eta} = -\Omega \times \eta, \tag{10a}$$
$$\dot{V}_a = -\Omega \times V_a + g\eta + a, \tag{10b}$$
$$y_{\mathrm{a}} = B^{\top}V_a. \tag{10c}$$

It is important to note that with a multiprobe Pitot tube, having $m \geq 3$ probes arranged so that $\mathrm{rank}(B) = 3$ simplifies the process. In such cases, one directly obtains measurements of V_a using the pseudo-inverse of B, enabling the application of velocity-aided attitude observers found in the existing literature, which are often based on Extended Kalman filtering techniques [13] or on constructive observer design approaches [6], [7]. However, the challenge is when dealing with either a single Pitot tube or a multiprobe Pitot tube with just two probes, as this leads to a $\mathrm{rank}(B)$ of 1 or 2.

IV. Observer Design

By exploiting the fact that $\eta = R^{\top}e_3 \in \mathcal{S}^2$, we introduce a concept akin to the one proposed in [18] by defining $\hat{\eta} = \hat{R}^{\top}e_3 \in \mathcal{S}^2$, with $\hat{R} \in \mathbf{SO}(3)$ the estimate of R. This approach entails an over-parametrization of the estimation for $\hat{\eta}$ and requires an observer design on $\mathbf{SO}(3)$, subsequently followed by a projection onto $\mathcal{S}^2$ to get the estimate $\hat{\eta}$. This over-parametrization brings forth several distinct advantages, effectively circumventing potential challenges such as minimal parametrizations for the normal direction η (e.g., spherical coordinates) and artificial singularities that may arise when designing the estimator $\hat{\eta}$ directly in $\mathcal{S}^2$ space. Let us now consider the following observer dynamics:

$$\begin{cases} \dot{\hat{R}} = \hat{R}\Omega^{\times} - \Delta^{\times}\hat{R} \\ \dot{\hat{V}}_a = -\Omega \times \hat{V}_a + g\hat{R}^{\top}e_3 + a + \delta_v \end{cases} \tag{11}$$

where $\Delta, \delta_v \in \mathbb{R}^3$ are the innovation terms. The steps towards developing these terms will follow the Riccati observer framework described in [19].

Define the attitude and velocity errors as

$$\tilde{R} := R\hat{R}^\top,\ \tilde{v}_a := R(V_a - \hat{V}_a). \tag{12}$$

Combining (4), (10) and (11), yields

$$\dot{\tilde{R}}e_3 = \tilde{R}\Delta^\times e_3, \tag{13a}$$
$$\dot{\tilde{v}}_a = (I - \tilde{R})ge_3 - \tilde{R}\hat{R}\delta_v. \tag{13b}$$

Consider now the first order approximation of (13). From Rodrigues' formula relating $\tilde{R} \in \mathbf{SO(3)}$ to its corresponding unit quaternion $\tilde{\mathbf{q}} := (\tilde{q}_0, \tilde{q})$:

$$\tilde{R} = I_3 + 2\tilde{q}^\times(\tilde{q}_0 I_3 + \tilde{q}^\times), \tag{14}$$

one gets:

$$\tilde{R} = I_3 + \tilde{\lambda}^\times + O(|\tilde{\lambda}|^2), \tag{15}$$

with $\tilde{\lambda} := 2\,\mathrm{sign}(\tilde{q}_0)\tilde{q}$. From there, one can express the first-order approximation of (13) as follows:

$$\dot{\tilde{\lambda}} = \Delta + O(|\tilde{\lambda}||\Delta|), \tag{16a}$$
$$\dot{\tilde{v}}_a = ge_3^\times\tilde{\lambda} - \hat{R}\delta_v + O(|\tilde{\lambda}||\delta_v|) + O(|\tilde{\lambda}|^2). \tag{16b}$$

The above system indicates that the first order dynamics of $\tilde{v}_a$ and $\tilde{\lambda}_{1,2}$ (the first two components of $\tilde{\lambda}$) are independent of $\tilde{\lambda}_3$. Using the fact that $\hat{R}$ evolves on the compact manifold $\mathbf{SO}(3)$, the observer (11) is well-posed and leads to well-posed observer error dynamics (16), independently of the choice of Δ_3. Since Δ_3 only affects $\tilde{\lambda}_3$ at the first-order approximation, we set (without affecting the observer error dynamics) this correction term to zero ($\Delta_3 := 0$).

$$\begin{aligned}\dot{\tilde{\lambda}}_{1,2} &= [\Delta_1, \Delta_2]^\top + O(|\tilde{\lambda}||\Delta|),\\ \dot{\tilde{v}}_a &= ge_3^\times\begin{bmatrix}\tilde{\lambda}_{1,2}\\ 0\end{bmatrix} - \hat{R}\delta_v + O(|\tilde{\lambda}||\delta_v|) + O(|\tilde{\lambda}|^2).\end{aligned} \tag{17}$$

As for the output equation (5), the output error is the standard one: $\tilde{y}_\mathrm{a} := B^\top V_a - B^\top\hat{V}_a$ that we rewrite, using (15), as follows:

$$\begin{aligned}\tilde{y}_\mathrm{a} &= B^\top R^\top\tilde{v}_a = B^\top\hat{R}^\top\tilde{R}^\top\tilde{v}_a\\ &= B^\top\hat{R}^\top\tilde{v}_a + O(|\tilde{\lambda}||\tilde{v}_a|).\end{aligned} \tag{18}$$

By setting $y = \tilde{y}_\mathrm{a} \in \mathbb{R}^m$, $x = [x_1^\top, x_2^\top]^\top = [\tilde{\lambda}_{1,2}^\top, \tilde{v}_a^\top]^\top$, with $x_1 \in \mathfrak{B}_2^2$ (closed ball of $\mathbb{R}^2$ of radius 2) and $x_2 = \tilde{v}_a \in \mathbb{R}^3$, and $u = [\Delta_{1,2}^\top, -(\hat{R}\delta_v)^\top]^\top$, one can rewrite (16)-(18) as follows:

$$\begin{cases}\dot{x} = Ax + u + O(|x_1||u|) + O(|x_1|^2) & \text{(19a)}\\ y = C^\star(t)x & \text{(19b)}\end{cases}$$

with $A = \begin{bmatrix}0_{2\times3} & 0_{2\times2}\\ ge_3^\times & 0_{3\times2}\end{bmatrix}$, $C^\star(t) = \Pi^\star(t)\bar{C}$, with $\Pi^\star(t) = B^\top R^\top$, $\bar{C} = [0_{3\times2}\ I_3]$. Setting $C(t) = \Pi(t)\bar{C}$ with $\Pi(t) = B^\top\hat{R}^\top$ then yields

$$y = C(t)x + O(|x_1||x_2|). \tag{20}$$

Proposition 1: Consider the system dynamics (10) along with the observer dynamics (11). Assume that v_a is continuous and bounded and the signal inputs Ω, a are also bounded. Choose the innovation:

$$u = -PC^\top(t)Qy, \tag{21}$$

with $P \in \mathbb{S}_+(5)$ the symmetric positive definite matrix solution to the following Continuous Riccati (CRE) Equation

$$\begin{aligned}\dot{P} &= AP + PA^\top - PC^\top(t)QC(t)P + S,\\ P(0) &= P_0 \in \mathbb{S}_+(5)\end{aligned} \tag{22}$$

with $Q \in \mathbb{S}_+(m)$ and $S \in \mathbb{S}_+(5)$ constant symmetric positive definite matrices. If the measurement collection is persistently exciting, i.e., if $\Pi^\star(t)$ satisfies (3), then the origin of observer error (19a),(20) is locally exponentially stable.

Proof: Consider the following candidate Lyapunov function:

$$\mathcal{L} := \frac{1}{2}x^\top P^{-1}x.$$

From (19)-(22), one deduces:

$$\begin{aligned}\dot{\mathcal{L}} = &-\frac{1}{2}x^\top\big(C^\top(t)QC(t) + P^{-1}SP^{-1}\big)x\\ &+\frac{1}{2}x^\top P^{-1}(O(|x_1||u|) + O(|x|^2))\\ &+\frac{1}{2}(O(|x_1||u|) + O(|x|^2))^\top P^{-1}x.\end{aligned}$$

It is straightforward to see that the right hand side is locally negative definite as long as P is positive definite and well-conditioned. Since A is a real nilpotent matrix, one concludes that all its eigenvalues are zero. Using the fact that $C^\star(t) = \Pi^\star(t)\bar{C}$, one deduces that the pair $(A, \bar{C})$ is Kalman observable. This implies, using Lemma 1, that the equilibrium $x = 0$ of (19) is uniformly observable if $\Pi^\star(t)$ is persistently exciting in the sense of (3). From there, one deduces that the Riccati solution at the equilibrium point (i.e., when $C(t) = C^\star(t)$) is bounded and well-conditioned (see [20], [21]). Combining this with the fact that $C(t)$ is uniformly continuous, one shows by continuity (see Theorem 3.1 and Corollary 3.2 [22]) that $P(t)$ (solution of (22)) and $P^{-1}(t)$ remain bounded along the solutions to the systems (19a),(20) and (21)-(22) w.r.t. initial conditions taken in a small neighborhood of $x = 0$. From there, one concludes that $\mathcal{L}$ converges exponentially to zero. ∎

The above proposition indicates that to be able to obtain an exponentially stable estimate of the air velocity and the gravitational direction, one either has to use a multiprobe Pitot tube with $m \geq 3$ probes to guarantee that B is full rank or impose a trajectory that introduces some persistence of excitation on pitch and yaw when considering a single Pitot tube $b_1 = e_1$. Note that only a persistent motion on the yaw (respectively pitch) is required when considering multiprobe Pitot tube with two probes such that $b_1, b_2 \in \mathrm{span}\{e_1, e_3\}$ (respectively $b_1, b_2 \in \mathrm{span}\{e_1, e_2\}$).

Based on the estimate $\hat{V}_a$ of V_a when the uniform observability condition (3) is fulfilled, one can reasonably get

the estimates of the airspeed $\mathbf{V}_a$, angle-of-attack α and the side-slip angle β from the well-known polar representation $V_a = \mathbf{V}_a[c_\alpha c_\beta, c_\alpha s_\beta, s_\alpha]^\top$. From there, one deduces the airspeed estimate $\hat{\mathbf{V}}_a = |\hat{V}_a|$, and the angles

$$\hat{\alpha} = \arcsin\left(\frac{\hat{V}_{a,3}}{|\hat{V}_a|}\right), \ \hat{\beta} = \arctan\left(\frac{\hat{V}_{a,2}}{\hat{V}_{a,1}}\right).$$

V. Experimental results

This section presents the results of the proposed observer design, which was evaluated using real flight data acquired from an indoor flight experiment involving the Eflite Convergence VTOL UAV. The observer was implemented in a discretized version. The vehicle is equipped with the *Pixhawk 4* microcontroller running the PX4 autopilot [23]. The *Pixhawk 4* incorporates an IMU, providing measurements for the specific acceleration and angular velocity.

Additionally, it features an external 3-axis magnetometer, a GNSS receiver that provides position and inertial velocity data, and a Pitot tube aligned with $e_1^{\mathcal{B}}$ (i.e., $B = e_1$), involving the *SDP33 Sensirion* differential-pressure sensor [24].

The autopilot records flight logs for each sensor. It maintains an on-board attitude and inertial velocity estimate (here denoted $\bar{R}$ and $\bar{v}$, respectively) computed by an Extended Kalman filter, known as *EKF2* [25].

The assumption that the absence of wind holds in the controlled indoor environment reasonably implies that the inertial velocity is equivalent to the air velocity ($v \approx v_a$). Consequently, the onboard inertial velocity estimate $\bar{V} := \bar{R}^\top \bar{v}$ becomes a valuable benchmark for assessing the accuracy of the air velocity estimate $\hat{V}_a \in \mathcal{B}$. Simultaneously, the onboard estimated attitude is used as a reference for evaluating the proposed filter's estimate of η by computing $\bar{\eta} := \bar{R}^\top e_3$. To assert the reliability of the onboard attitude and inertial velocity estimates in this experiment, we computed the first component of the body-fixed frame velocity estimate (i.e., $\bar{V}_1 = e_1^\top \bar{R}^\top \bar{v}$) and compared it to the Pitot tube measures $V_{a,1}$. The segment of the flight selected for this analysis is depicted in Fig. 1. It is shown that the measurements of $V_{a,1}$ and $\bar{V}_1$ differ mainly when $\bar{V}_1$ approaches zero, while for the remaining part of the flight, the differences are, at most, $1m/s$.

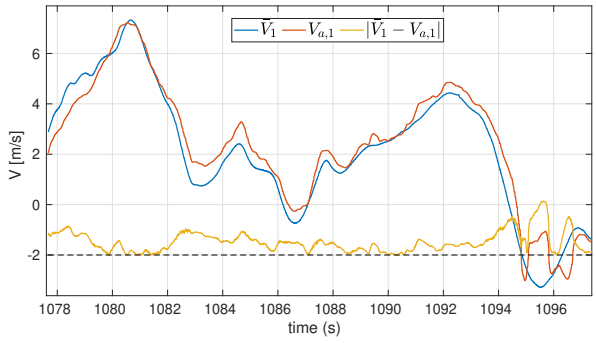

Fig. 1. Comparison between measurements of $V_{a,1}$ and the first component of the velocity in the body-fixed frame $\bar{V}_1$ in the real flight data set.

In this application using real data, the initialization was performed during a specific flight portion for which the p.e. condition (3) is satisfied to ensure uniform observability assessed here by the computation of the condition number of the matrix

$$\bar{M}(t_k, t_{k+1}) := \int_{t_k}^{t_{k+1}} \bar{R}(s) B B^\top \bar{R}^\top(s) ds, \qquad (23)$$

over the time interval, with $t_k = k\delta$, $k \in \mathbb{N}^*$ and $\delta = 2s$. The initial conditions at $t_0 = 1077.8s$ are such that:

$$\bar{V}(t_0) \approx [5, -1, 1.3]^\top (m/s), \ \hat{V}_a(t_0) = [10, -2, 0.3]^\top (m/s),$$
$$\bar{\eta}(t_0) \approx [0.30, -0.02, 0.96], \ \hat{\eta}(t_0) = \hat{R}^\top(t_0) e_3,$$

where $\hat{R}(t_0)$ is chosen using the Euler angle parametrization with a pitch of $-\pi/18$, a roll of $\pi/9$, and a yaw of zero. The matrix $P(t_0)$ is set to $\text{diag}(0.6I_2, 50I_3)$ and the matrices Q and S are set to 800 and $\text{diag}(0.01I_2, 0.2I_3)$, respectively. The sensor measurements were discretized with an update frequency of $250Hz$ for the IMU and $50Hz$ for the Pitot tube.

Fig. 2 shows the time evolution of the error terms $|\bar{\eta} - \hat{\eta}|$ and $|\bar{V} - \hat{V}_a|$ along with the condition number $\text{cond}(\bar{M})$. One remarks that the estimates $(\hat{\eta}, \hat{V}_a)$ reach practical convergence relative to the onboard estimates $(\bar{\eta}, \bar{V})$. The slight increase in errors observed in the time interval $[1091s, 1095s]$ is due to the notable rise in the condition number of $\bar{M}$. In contrast, during the time interval between $[1095s, 1098s]$, the slight increase is mainly due to the growing disparities between $\bar{V}_1$ and $V_{a,1}$, which become more pronounced as the Pitot tube measurements approach zero (see Fig. 1).

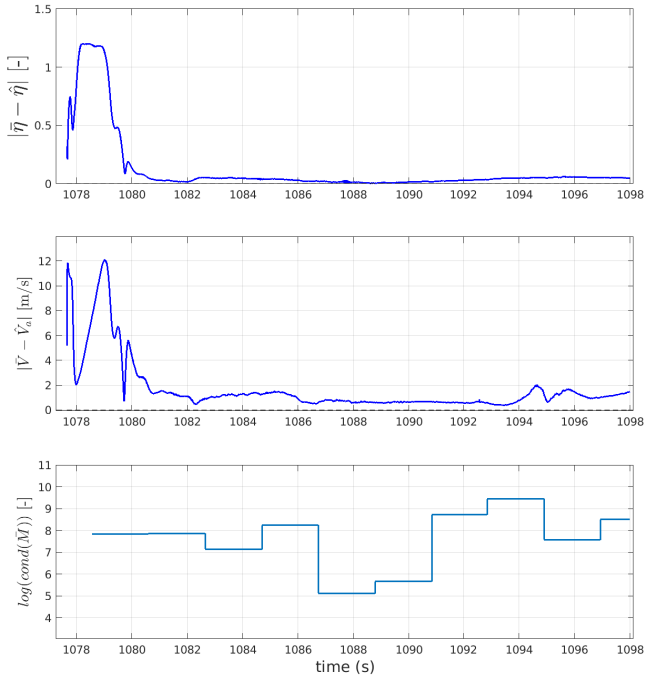

Fig. 2. Results for the experiment using real data. On the first and second plots, $|\bar{\eta} - \hat{\eta}|$ and $|\bar{V} - \hat{V}_a|$, respectively. The last plot shows the evolution $\text{cond}(\bar{M})$ over time.

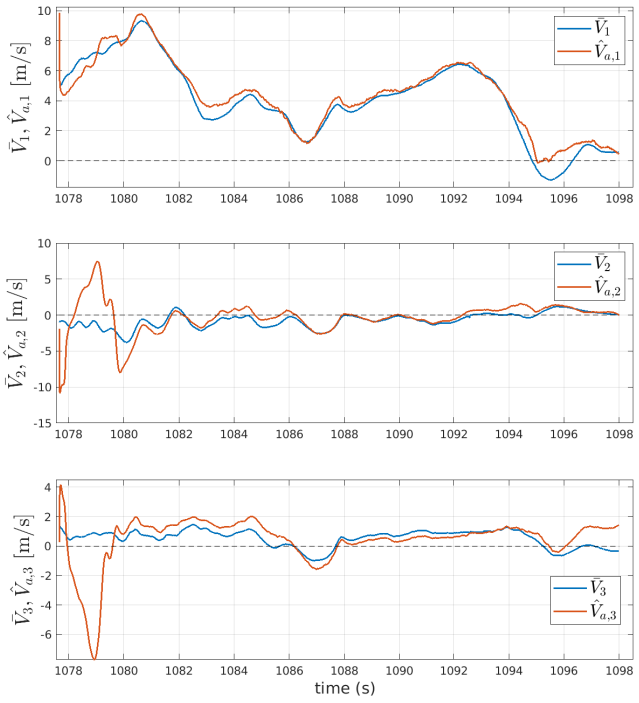

Fig. 3. Evolution of the air velocity estimate using real data. The plots compare the respective components of the estimated air velocity $\hat{V}_a$ (red) and the onboard estimated body-fixed frame velocity $\bar{V}$ (blue).

VI. Concluding Remarks

This paper presents a novel observer design for Pitot Tube-Assisted Air Velocity and Attitude Estimation in GNSS-Denied Environments. This approach is particularly valuable when dealing with small fixed-wing UAVs where traditional sensors used in attitude estimation, such as magnetometers or GNSS, are unreliable or unavailable. To the authors' knowledge, this design is the first to feature such stability properties. Realistic simulation and preliminary experimental tests exemplifying the common case of an aircraft with one Pitot tube illustrate the estimator's performance and applicability in typical aircraft trajectories.

Acknowledgment

This work has been supported by the ANR-ASTRID Project ASCAR and the Franco-Australian International Research Project "Advancing Autonomy for Unmanned Robotic Systems" (IRP ARS).

References

[1] R. Mahony, T. Hamel, and J.-M. Pflimlin, "Nonlinear complementary filters on the special orthogonal group," *IEEE Transactions on automatic control*, vol. 53, no. 5, pp. 1203–1218, 2008.

[2] P. Martin and E. Salaün, "Design and implementation of a low-cost observer-based attitude and heading reference system," *Control engineering practice*, vol. 18, no. 7, pp. 712–722, 2010.

[3] J.-M. Pflimlin, P. Binetti, P. Soueres, T. Hamel, and D. Trouchet, "Modeling and attitude control analysis of a ducted-fan micro aerial vehicle," *Control Engineering Practice*, vol. 18, no. 3, pp. 209–218, 2010.

[4] M.-D. Hua, G. Ducard, T. Hamel, R. Mahony, and K. Rudin, "Implementation of a nonlinear attitude estimator for aerial robotic vehicles," *IEEE Transactions on Control Systems Technology*, vol. 22, no. 1, pp. 201–213, 2013.

[5] G. Troni and L. L. Whitcomb, "Preliminary experimental evaluation of a doppler-aided attitude estimator for improved doppler navigation of underwater vehicles," in *2013 IEEE International Conference on Robotics and Automation*. IEEE, 2013, pp. 4134–4140.

[6] M.-D. Hua, P. Martin, and T. Hamel, "Stability analysis of velocity-aided attitude observers for accelerated vehicles," *Automatica*, vol. 63, pp. 11–15, 2016.

[7] M. Benallegue, A. Benallegue, R. Cisneros, and Y. Chitour, "Velocity-aided imu-based attitude estimation," *arXiv preprint arXiv:2002.10205*, 2020.

[8] M. Wang and A. Tayebi, "Nonlinear attitude estimation using intermittent linear velocity and vector measurements," in *2021 60th IEEE Conference on Decision and Control (CDC)*. IEEE, 2021, pp. 4707–4712.

[9] P. van Goor, T. Hamel, and R. Mahony, "Constructive equivariant observer design for inertial velocity-aided attitude," *IFAC-PapersOnLine*, vol. 56, no. 1, pp. 349–354, 2023.

[10] F. A. P. Lie, "Synthetic air data estimation," Ph.D. dissertation, university of minnesota, 2014.

[11] K. T. Borup, T. I. Fossen, and T. A. Johansen, "A nonlinear model-based wind velocity observer for unmanned aerial vehicles," *IFAC-PapersOnLine*, vol. 49, no. 18, pp. 276–283, 2016.

[12] K. Sun, C. D. Regan, and D. Gebre-Egziabher, "Observability and performance analysis of a model-free synthetic air data estimator," *Journal of Aircraft*, vol. 56, no. 4, pp. 1471–1486, 2019.

[13] T. A. Johansen, A. Cristofaro, K. Sørensen, J. M. Hansen, and T. I. Fossen, "On estimation of wind velocity, angle-of-attack and sideslip angle of small uavs using standard sensors," in *2015 International Conference on Unmanned Aircraft Systems (ICUAS)*. IEEE, 2015, pp. 510–519.

[14] R. Mahony, M. Euston, J. Kim, P. Coote, and T. Hamel, "A non-linear observer for attitude estimation of a fixed-wing unmanned aerial vehicle without gps measurements," *Transactions of the Institute of Measurement and Control*, vol. 33, no. 6, pp. 699–717, 2011.

[15] T. Hamel and C. Samson, "Position estimation from direction or range measurements," *Automatica*, vol. 82, pp. 137–144, 2017.

[16] P. van Goor, T. Hamel, and R. Mahony, "Equivariant filter (eqf)," *IEEE Transactions on Automatic Control*, 2022.

[17] C.-T. Chen, *Linear system theory and design*. Saunders college publishing, 1984.

[18] M.-D. Hua and G. Allibert, "Riccati observer design for pose, linear velocity and gravity direction estimation using landmark position and imu measurements," in *2018 IEEE Conference on Control Technology and Applications (CCTA)*. IEEE, 2018, pp. 1313–1318.

[19] M.-D. Hua, T. Hamel, and C. Samson, "Riccati nonlinear observer for velocity-aided attitude estimation of accelerated vehicles using coupled velocity measurements," in *2017 IEEE 56th Annual Conference on Decision and Control (CDC)*. IEEE, 2017, pp. 2428–2433.

[20] G. Besançon, *Nonlinear observers and applications*. Springer, 2007, vol. 363.

[21] T. Hamel and C. Samson, "Riccati observers for position and velocity bias estimation from either direction or range measurements," *arXiv preprint arXiv:1606.07735*, 2016.

[22] ——, "Riccati observers for the nonstationary pnp problem," *IEEE Transactions on Automatic Control*, vol. 63, no. 3, pp. 726–741, 2017.

[23] L. Meier, D. Honegger, and M. Pollefeys, "Px4: A node-based multithreaded open source robotics framework for deeply embedded platforms," in *2015 IEEE international conference on robotics and automation (ICRA)*. IEEE, 2015, pp. 6235–6240.

[24] *Preliminary Datasheet SDP33*, Sensirion, 2017, version 0.1.

[25] "Using the ECL EKF — PX4 User Guide (v1.12) — docs.px4.io," https://docs.px4.io/v1.12/en/advanced_config/tuning_the_ecl_ekf.html, [Accessed 25-03-2024].